Centrality dependences of the pseudorapidity distributions of charged particles in Au+Au collisions at RHIC energies*

JIANG Zhi-Jin(姜志进)[1)] SUN Yu-Fen(孙玉芬) NI Wei-Xin(倪卫新)

Science College, Shanghai Science and Technology University, Shanghai 200093, China

Abstract By employing the Glauber model, we give the centrality dependences of the numbers of participants and binary nucleon-nucleon collisions in nucleus-nucleus collisions. By taking into account the energy loss of the participants in their multiple collisions, we then present the pseudorapidity distributions of charged particles in nucleus-nucleus collisions as a function of beam energy and impact parameter. Finally, we analyze the centrality dependence of the pseudorapidity of the charged particles in Au+Au collisions at energies from $\sqrt{s_{\rm NN}}$=19.6 to 200 GeV. The theoretical results are in good agreement with the experimental observations of the RHIC-PHOBOS collaboration.

Key words Glauber model, spectators, binary nucleon-nucleon collisions, pseudorapidity distributions

PACS 25.75.Dw

1 Introduction

The pseudorapidity distributions of charged particles in heavy-ion These interactions can be obtained directly from experiments. These then provides a feasible approach for studying the mechanism and process of particle production in nucleus-nucleus collisions. According to Bjorken's theory [1], the energy density of the initial matter produced by two colliding nuclei is proportional to $\mathrm{d}N/\mathrm{d}y$, where N is the charge multiplicity and y is the rapidity. In addition, the pseudorapidity distributions are related to the freeze-out temperature [2, 3] if the matter generated in a heavy-ion collision is in thermal equilibrium at the time of freeze-out. The investigations of pseudorapidity distributions may help us to find out the energy density or temperature of the matter obtained in nucleus-nucleus collisions. This is important for studying phase transition conditions and searching for the quark gluon plasma (QGP). Hence, the pseudorapidity distributions of charged particles in heavy-ion collisions are one of the most important subjects in high-energy experimental and theoretical investigations.

In recent years, collaborations at RHIC (Relativistic Heavy Ion Collider) have made many measurements of pseudorapidity distributions of charged particles in nucleus-nucleus collisions [4–12]. The measurements show that, for certain centrality collisions, the distribution exhibits a plateau in the mid-pseudorapidity region with a depression around $\eta = 0$. With the increase in the centrality (or impact parameter), the plateau becomes wide and low. In order to understand these observations, various theoretical models have been put forward. Typical examples include the hydrodynamic model [13–15], the three-fireball model [16, 17], the thermalized model [2, 3], the thermalized cylinder model [18], the quark recombination model [19, 20] and the transport model [21, 22]. In our previous work [23], we discussed the pseudorapidity distributions of charged particles in Au+Au collisions at $\sqrt{s_{\rm NN}}$=200 GeV. In this paper, we will generalize our theoretical model to nucleus-nucleus collisions at any beam energies and centrality cuts.

The paper is organized as follows. Firstly, by using the Glauber model [24, 25], we present the analytic forms for the numbers of participants and binary

Received 9 October 2009

* Supported by Key Foundation of Shanghai (S30501)

1) E-mail: Jzj265@163.com

nucleon-nucleon collisions as a function of the impact parameter in heavy-ion interactions. We then give the beam energy and centrality dependences of the pseudorapidity distributions of charged particles in nucleus-nucleus collisions after considering the energy loss of the participants in their multiple collisions. Finally, by making use of the constructed model, we analyze the experimental measurements of the RHIC-PHOBOS collaboration in different centrality Au + Au collisions at energies of $\sqrt{s_{\rm NN}}$=19.6 to 200 GeV.

2 The numbers of participants and binary nucleon-nucleon collisions in heavy-ion collisions

In high-energy nucleus-nucleus collisions, the two nuclei will penetrate each other. In this process the nucleons in one nucleus will collide with those of the other one. Here, for the sake of completeness and later application, we will, based on the Glauber model, discuss the number of participants and binary nucleon-nucleon collisions in heavy-ion collisions.

2.1 The number of participants in heavy-ion collisions

The nucleon distribution in a nucleus with mass number A is usually taken to be a Wood-Saxon distribution

$$\rho(r)=\frac{\rho_0}{1+\exp[(r-r_0)/a]}, \tag{1}$$

where r_0 is the radius of the nucleus and a is the diffuseness parameter. Different values for these two constants have been employed in different papers [26, 27]. ρ_0 in Eq. (1) is a normalization constant determined by condition

$$\int_V \rho(r)\mathrm{d}V = A.$$

Here, we take [27] $r_0 = 1.19\ A^{1/3} - 1.61\ A^{-1/3}$ and a= 0.54 fm. For Au, A=197, r_0=6.65 fm and $\rho_0 = 0.15/\mathrm{fm}^3$.

From the nuclear density $\rho(r)$ we obtain the nuclear thickness function:

$$T(\boldsymbol{s})=\int\rho(\boldsymbol{s},z)\mathrm{d}z. \tag{2}$$

This represents the nucleon number in the tube with unit bottom area located at position $\boldsymbol{s}$ relative to the center of the nucleus, as shown in Fig. 1.

Let us consider an A-B nuclear collision with impact parameter $\boldsymbol{b}$ (cf Fig. 2). Given that the total nucleon-nucleon inelastic cross section is $\sigma_{\rm NN}^{\rm in}$, it follows that $\sigma_{\rm NN}^{\rm in}T_{\rm B}(\boldsymbol{s}-\boldsymbol{b})$ is the number of nucleons that

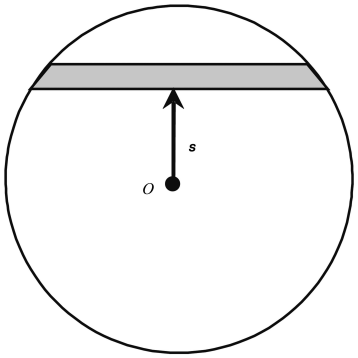

Fig. 1. The tube with unit bottom area located at position $\boldsymbol{s}$ with respect to the center of the nucleus.

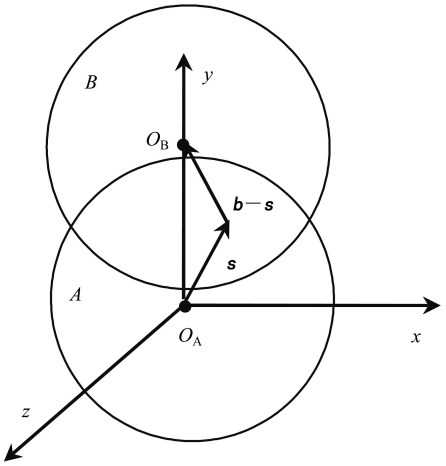

Fig. 2. An A-B nuclear collision with impact parameter $\boldsymbol{b}$.

a nucleon of nucleus A at position $\boldsymbol{s}$ will encounter during the process as it passes through nucleus B. Then the probability that this nucleon survives the collisions is $\exp[-\sigma_{\rm NN}^{\rm in}T_B(\boldsymbol{s}-\boldsymbol{b})]$, and the probability that it undergoes collisions is $1-\exp[-\sigma_{\rm NN}^{\rm in}T_B(\boldsymbol{s}-\boldsymbol{b})]$. Hence,

$$n_A(\boldsymbol{b},\boldsymbol{s})=T_A(\boldsymbol{s})\{1-\exp[-\sigma_{\rm NN}^{\rm in}T_B(\boldsymbol{s}-\boldsymbol{b})]\}$$

stands for the number of participants in nucleus A in the tube parallel to the collision axis with unit bottom area at position $\boldsymbol{s}$. Similarly, the number of participants in nucleus B is

$$n_B(\boldsymbol{b},\boldsymbol{s})=T_B(\boldsymbol{s}-\boldsymbol{b})\{1-\exp[-\sigma_{\rm NN}^{\rm in}T_A(\boldsymbol{s})]\},$$

and the total number of participants in the considered tube is

$$\begin{aligned} n_{\rm Part}(\boldsymbol{b},\boldsymbol{s}) \;=\; & n_A(\boldsymbol{b},\boldsymbol{s})+n_B(\boldsymbol{b},\boldsymbol{s})= \\ & T_A(\boldsymbol{s})\{1-\exp[-\sigma_{\rm NN}^{\rm in}T_B(\boldsymbol{s}-\boldsymbol{b})]\}+ \\ & T_B(\boldsymbol{s}-\boldsymbol{b})\{1-\exp[-\sigma_{\rm NN}^{\rm in}T_A(\boldsymbol{s})]\}. \end{aligned}$$

Accordingly, in an A-B nuclear collision with impact parameter $\boldsymbol{b}$, the total number of participants is

$$N_{\rm Part}(\boldsymbol{b}) = \int n_{\rm Part}(\boldsymbol{b},\boldsymbol{s})\mathrm{d}^2\boldsymbol{s} = \int_{-\sqrt{r^2-\frac{b^2}{4}}}^{\sqrt{r^2-\frac{b^2}{4}}}\mathrm{d}x\int_{b-\sqrt{r^2-x^2}}^{\sqrt{r^2-x^2}} n_{\rm Part}(\boldsymbol{b},\boldsymbol{s})\mathrm{d}y.$$

Then, for a collision with a certain centrality cut, the mean number of participants is given by

$$\bar{N}_{\rm Part} = \frac{\int N_{\rm Part}(\boldsymbol{b})\mathrm{d}^2\boldsymbol{b}}{\int \mathrm{d}^2\boldsymbol{b}}. \tag{3}$$

Table 1. The regions of impact parameter $\boldsymbol{b}$, the mean number of participants $\bar{N}_{\rm Part}$ and the mean numbers of binary nucleon-nucleon collisions $\bar{N}_{\rm NN}$ in five centrality cuts in Au+Au collisions at $\sqrt{s_{\rm NN}}$=19.6, 62.4, 130 and 200 GeV. The values with (without) errors are the results from the RHIC-PHOBOS collaboration [4, 7] (there are no data for $\bar{N}_{\rm NN}$ for $\sqrt{s_{\rm NN}}$=19.6 and 130 GeV) or Eq. (3) and Eq. (10), respectively.

centrality cuts (%)	b/fm	$\bar{N}^{19.6}_{\rm Part}$		$\bar{N}^{19.6}_{\rm NN}$		$\bar{N}^{62.4}_{\rm Part}$		$\bar{N}^{62.4}_{\rm NN}$	
0–6	0–3.63	333.5	337±12	781.3	–	336.9	335±11	853.8	883±65
6–15	3.63–5.74	257.4	265±11	560.3	–	261.1	266±9	612.3	643±48
15–25	5.74–7.41	186.1	194±12	368.5	–	189.5	189±9	402.7	402±36
25–35	7.41–8.77	129.9	138±13	230.7	–	132.9	130±10	237.6	240±30
35–45	8.77–9.94	87.8	–	137.7	–	90.2	86±9	150.4	136±22
centrality cuts (%)	b/fm	$\bar{N}^{130}_{\rm Part}$		$\bar{N}^{130}_{\rm NN}$		$\bar{N}^{200}_{\rm Part}$		$\bar{N}^{200}_{\rm NN}$	
0–6	0–3.63	340.8	340±11	970.7	–	341.5	344±11	994.3	1040±77
6–15	3.63–5.74	266.0	275±9	696.1	–	266.5	274±9	713.1	762±57
15–25	5.74–7.41	193.9	196±8	457.9	–	194.7	200±8	469.1	483±40
25–35	7.41–8.77	136.8	136±6	286.6	–	137.5	138±6	293.6	286±25
35–45	8.77–9.94	93.4	90±5	171	–	94.0	93±5	175.2	164±15

Table 1 shows the mean number of participants $\bar{N}_{\rm Part}$ in Au+Au collisions at $\sqrt{s_{\rm NN}}$=19.6, 62.4, 130 and 200 GeV, respectively, for five centrality cuts. In the calculations, $\sigma^{\rm in}_{\rm NN}$ is taken to be [6] 33, 36, 41 and 42 mb while the energies change from low to high. The numbers with (without) errors are the results from the RHIC-PHOBOS collaboration [4, 7] or Eq. (3), respectively. From Table 1 we see that the calculations from Eq. (3) are in good agreement with the results from the RHIC-PHOBOS collaboration.

2.2 The numbers of binary nucleon-nucleon collisions in heavy-ion collisions

In order to get the numbers of binary nucleon-nucleon collisions, we first divide Eq. (1) by the nuclear mass number A:

$$\rho_{\rm P}(r) = \frac{\rho_0}{A\{1+\exp[(r-r_0)/a]\}}. \tag{4}$$

It is evident that the above equation represents the probability density of the nucleon distribution, that is, the probability of finding a nucleon in the unit volume. It certainly satisfies the condition of normalization:

$$\int \rho_{\rm P}(r)\mathrm{d}V = 1.$$

In terms of $\rho_{\rm P}(r)$, we have another kind of nuclear thickness function:

$$T_{\rm P}(\boldsymbol{s}) = \int \rho_{\rm P}(\boldsymbol{s},z)\mathrm{d}z,$$

which is normalized according to

$$\int T_{\rm P}(\boldsymbol{s})\mathrm{d}^2\boldsymbol{s} = 1.$$

Obviously, $T_{\rm P}(\boldsymbol{s})$ is the probability of finding a nucleon in the tube, as shown in Fig. 1. Then, in an A-B nuclear collision with impact parameter $\boldsymbol{b}$, the probability of a nucleon-nucleon collision in a unit area with normal direction parallel to the collision axis has the form

$$T_{\rm P}(\boldsymbol{b}) = \int T_{{\rm P}A}(\boldsymbol{s})T_{{\rm P}B}(\boldsymbol{s}-\boldsymbol{b})\mathrm{d}^2\boldsymbol{s}, \tag{5}$$

which is normalized as

$$\int T_{\rm P}(\boldsymbol{b})\mathrm{d}^2\boldsymbol{b} = 1.$$

Then the probability of a nucleon-nucleon inelastic collision is $T_P(\boldsymbol{b})\sigma^{\rm in}_{\rm NN}$ and the probability of having a nucleon-nucleon inelastic collision n times is given by

$$P(n,\boldsymbol{b}) = \left(\begin{array}{c} AB \\ n \end{array}\right)[T_{\rm P}(\boldsymbol{b})\sigma^{\rm in}_{\rm NN}]^n[1-T_{\rm P}(\boldsymbol{b})\sigma^{\rm in}_{\rm NN}]^{AB-n}, \tag{6}$$

which meets the normalization

$$\sum_{n=0}^{AB} P(n,\boldsymbol{b}) = 1.$$

The number of binary nucleon-nucleon inelastic collisions in an A-B nucleus-nucleus collision at impact parameter $\boldsymbol{b}$ can then be written as

$$N_{\rm NN}(\boldsymbol{b}) = \frac{\sum_{n=1}^{AB} nP(n,\boldsymbol{b})}{\sum_{n=1}^{AB} P(n,\boldsymbol{b})}, \tag{7}$$

where

$$\sum_{n=1}^{AB} P(n,\boldsymbol{b}) = \sum_{n=0}^{AB} P(n,\boldsymbol{b}) - P(0,\boldsymbol{b}) = 1-[1-T_{\rm P}(\boldsymbol{b})\sigma_{\rm NN}^{\rm in}]^{AB}$$

and

$$\sum_{n=1}^{AB} nP(n,\boldsymbol{b}) = ABT_{\rm P}(\boldsymbol{b})\sigma_{\rm NN}^{\rm in}. \tag{8}$$

Inserting this into Eq. (7), we get

$$N_{\rm NN}(\boldsymbol{b}) = \frac{ABT_{\rm P}(\boldsymbol{b})\sigma_{\rm NN}^{\rm in}}{1-[1-T_{\rm P}(\boldsymbol{b})\sigma_{\rm NN}^{\rm in}]^{AB}}. \tag{9}$$

The mean number of binary nucleon-nucleon collisions in a certain impact parameter region (or centrality cut region) is then given by

$$\bar{N}_{\rm NN} = \frac{\int N_{\rm NN}(\boldsymbol{b})\mathrm{d}^2\boldsymbol{b}}{\int \mathrm{d}^2\boldsymbol{b}}. \tag{10}$$

Table 1 shows the mean number of binary nucleon-nucleon collisions $\overline{N}_{\rm NN}$ in five centrality cuts in Au+Au collisions at $\sqrt{s_{\rm NN}}$=19.6, 62.4, 130 and 200 GeV, respectively. The numbers with (without) errors are the results from the RHIC-PHOBOS collaboration [7] (there are no data for $\sqrt{s_{\rm NN}}$=19.6 and 130 GeV) or Eq. (10), respectively. From Table 1 we see that the calculations from Eq. (10) are in good agreement with the results given by the RHIC-PHOBOS collaboration.

3 Pseudorapidity distributions of charged particles in nucleus-nucleus collisions

In nucleus-nucleus collisions the energy of a participant decreases when increasing the number of collisions with other participants. The lost energy is accumulated in the region around the center of mass and finally freezes to the measurable particles in the final state. It is obvious that the total number of charged particles in a nucleus-nucleus collision is the sum of those generated in each nucleon-nucleon collision. Therefore, the rapidity distribution of the charged particles in a nucleus-nucleus collision at impact parameter $\boldsymbol{b}$ can be expressed as the weighted superposition of the distributions in binary nucleon-nucleon collisions:

$$\frac{\mathrm{d}N_{AB}(\boldsymbol{b})}{\mathrm{d}y} = \sum_{n=1}^{AB} P(n,\boldsymbol{b}) \sum_{i=1}^{n} \frac{\mathrm{d}N_{\rm NN}(\sqrt{s_{\rm NN}^i},\boldsymbol{b})}{\mathrm{d}y}, \tag{11}$$

where $P(n,\boldsymbol{b})$ is given by Eq. (6), $\sqrt{s_{\rm NN}^i}$ is the c.m.s. energy in the ith nucleon-nucleon collision and $\mathrm{d}N_{\rm NN}\left(\sqrt{s_{\rm NN}^i},\boldsymbol{b}\right)/\mathrm{d}y$ is the corresponding rapidity distribution, which in this paper is taken to be [28]

$$\frac{\mathrm{d}N_{\rm NN}(\sqrt{s_{\rm NN}},\boldsymbol{b})}{\mathrm{d}y} = \frac{C\left(\sqrt{s_{\rm NN}}\right)}{1+\exp\left[\dfrac{|y(\boldsymbol{b}|-y_0\left(\sqrt{s_{\rm NN}}\right)}{\Delta\left(\sqrt{s_{\rm NN}}\right)}\right]}, \tag{12}$$

where $\Delta(\sqrt{s_{\rm NN}})$, $C\left(\sqrt{s_{\rm NN}}\right)$ and $y_0\left(\sqrt{s_{\rm NN}}\right)$ determine the width, height and peak position of the rapidity distribution, respectively. They are all functions of $\sqrt{s_{\rm NN}}$, and in this article are taken as

$$\Delta\left(\sqrt{s_{\rm NN}}\right) = 0.034\ln(\sqrt{s_{\rm NN}})+0.472,$$

$$C(\sqrt{s_{\rm NN}}) = 0.309\ln(\sqrt{s_{\rm NN}})+0.841,$$

$$y_0(\sqrt{s_{\rm NN}}) = 0.706\ln(\sqrt{s_{\rm NN}})+0.009.$$

The relation between the rapidity and the pseudorapidity is given by

$$y(\boldsymbol{b}) = \frac{1}{2}\ln\left[\frac{\sqrt{p_{\rm T}^2(\boldsymbol{b})\cosh^2\eta+m^2}+p_{\rm T}(\boldsymbol{b})\sinh\eta}{\sqrt{p_{\rm T}^2(\boldsymbol{b})\cosh^2\eta+m^2}-p_{\rm T}(\boldsymbol{b})\sinh\eta}\right] \tag{13}$$

and

$$\frac{\mathrm{d}N_{AB}(\boldsymbol{b})}{\mathrm{d}\eta} = \sqrt{1-\frac{m^2}{m_{\rm T}^2\cosh^2 y}}\,\frac{\mathrm{d}N_{AB}(\boldsymbol{b})}{\mathrm{d}y}. \tag{14}$$

Experimental investigations [29] have shown that the transverse momentum of the charged particles increases as the impact parameter $\boldsymbol{b}$ decreases. Thus, in Eq. (12) the rapidity distribution of the nucleon-nucleon collisions depends on the impact parameter $\boldsymbol{b}$ of the nucleus-nucleus collisions.

Figure 3 shows the pseudorapidity distributions of the charged particles in p+p collisions at $\sqrt{s}$=23.6, 45.2 and 200 GeV, counting from bottom to top. The circles, triangles and solid circles are the experimental measurements of the UA5 collaboration [30–32]. The solid lines are the numerical results from Eq. (12). It

can be seen from this figure that Eq. (12) represents the experimental observations well.

In the above calculations, the m in Eqs. (13) and (14) is taken to be the mean value of the masses of the pion, kaon and proton. These three kinds of particles constitute the overwhelming majority of the charged particles in the final state with frequencies of about 84%, 12% and 4 %, respectively [29]. The transverse momentum $p_{\rm T}$ in Eqs. (13) and (14) takes on the values of 0.20, 0.25 and 0.35 GeV/c in accordance with the increasing c.m.s energies.

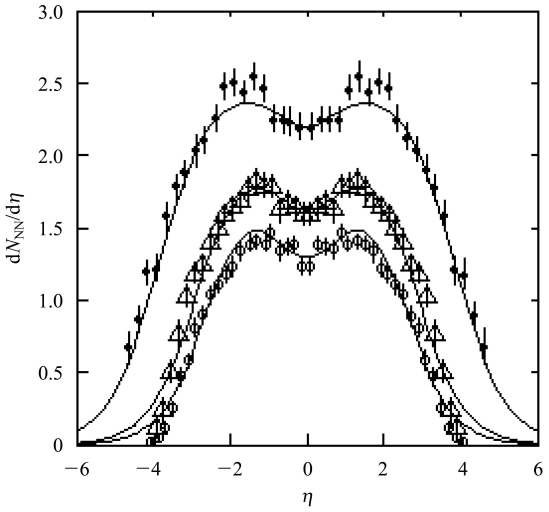

Fig. 3. Pseudorapidity distributions of charged particles in p+p collisions at $\sqrt{s}$=23.6, 45.2 and 200 GeV, counting from bottom to top. The circles, triangles and solid circles are the results from the UA5 collaboration [30–32]. The solid lines are the numerical results from Eq. (12).

In order to get the rapidity distribution from Eq. (11), we need to know the c.m.s. energy in each nucleon-nucleon collision $\sqrt{s^i_{\rm NN}}(i{=}1,\ 2\cdots N_{\rm NN}(\boldsymbol{b}))$. However, the functional relation between $\sqrt{s^i_{\rm NN}}$ and i is not yet clear. To deal with this problem, we may first ignore the differences in c.m.s. energy for different nucleon-nucleon collisions. Such as in Au+Au collisions at $\sqrt{s_{\rm NN}}$ = 200 GeV, we may just take $\sqrt{s^i_{\rm NN}}=\sqrt{s_{\rm NN}}=200$ GeV for all nucleon-nucleon collisions. Then, from Eqs. (8) and (9), Eq. (11) becomes

$$\frac{\mathrm{d}N_{AB}(\boldsymbol{b})}{\mathrm{d}y} \approx N_{\rm NN}(\boldsymbol{b})\{1-[1-T_{\rm P}(\boldsymbol{b})\sigma^{\rm in}_{\rm NN}]^{AB}\}\times \frac{\mathrm{d}N_{\rm NN}\left(\sqrt{s_{\rm NN}},\boldsymbol{b}\right)}{\mathrm{d}y}, \tag{15}$$

where, $T_{\rm P}(\boldsymbol{b})$ and $N_{\rm NN}(\boldsymbol{b})$ are given by Eqs. (5) and (9), respectively. However, in reality the energies of participants in different nucleon-nucleon collisions are different. The smaller the impact parameter, the larger is the number $N_{\rm NN}(\boldsymbol{b})$ (see Table 1) and the less is the mean c.m.s. energy available for each nucleon-nucleon collision due to a higher energy loss, and hence, the smaller is the contribution to the yield of charged particles. According to this, $\mathrm{d}N_{AB}(\boldsymbol{b})/\mathrm{d}y$ should decrease with $N_{\rm NN}(\boldsymbol{b})$. That is, under the assumption that the c.m.s. energies in all nucleon-nucleon collisions are the same, $\sqrt{s^i_{\rm NN}}=\sqrt{s_{\rm NN}}=$ 200 GeV, the actual numbers of nucleon-nucleon collisions contributing to the charged particle yield in the final state should be less than those listed in Table 1 or those given by Eq. (10). Thus, we introduce an attenuation factor $\beta(\boldsymbol{b})$, which is defined as

$$\beta(\boldsymbol{b})=1+\alpha(\boldsymbol{b})[N_{\rm NN}(\boldsymbol{b})-1], \tag{16}$$

where $\alpha(\boldsymbol{b})$ is a free parameter (the only free parameter used in our analysis), which can be fixed by fitting the experimental data. Then the yield of charged particles produced in a nucleus-nucleus collision should be determined by the number of effective nucleon-nucleon collisions:

$$N^{\rm eff}_{\rm NN}(\boldsymbol{b})=\frac{N_{\rm NN}(\boldsymbol{b})}{\beta(\boldsymbol{b})}, \tag{17}$$

and accordingly Eq. (15) should be modified as follows:

$$\frac{\mathrm{d}N_{AB}(\boldsymbol{b})}{\mathrm{d}y} = N^{\rm eff}_{\rm NN}(\boldsymbol{b})\{1-[1-T_{\rm P}(\boldsymbol{b})\sigma^{\rm in}_{\rm NN}]^{AB}\}\times \frac{\mathrm{d}N_{\rm NN}(\sqrt{s_{\rm NN}},\boldsymbol{b})}{\mathrm{d}y}. \tag{18}$$

For p+p collisions, $N_{\rm NN}(\boldsymbol{b})$= 1, then $\beta(\boldsymbol{b})=N^{\rm eff}_{\rm NN}(\boldsymbol{b})$ =1. Furthermore, it is known from Eq. (9) that $T_{\rm p}(\boldsymbol{b})\ \sigma^{\rm in}_{\rm NN}=1$ in this case. Thus, as expected, the above equation reduces to the rapidity distribution for p+p collisions.

Since the functional forms of $p_{\rm T}(\boldsymbol{b})$ in Eq. (13) and $\alpha(\boldsymbol{b})$ in Eq. (16) are at present not clearly known, the mean charge multiplicities in each centrality cut cannot be obtained by integrating over the impact parameter, as we do in Eqs. (3) and (10). Here we will adopt a common method, i.e. approximately using the charge multiplicities at the mid impact parameter in each centrality cut (cf Table 1) to stand for the mean charge multiplicities. Substituting Eq. (18) into Eq. (14), we can then use it to discuss the pseudorapidity distribution of charged particles in nucleus-nucleus collisions.

Figure 4 shows the centrality dependences of the pseudorapidity distributions of charged particles in Au+Au collisions at $\sqrt{s_{\rm NN}}$=19.6, 62.4, 130 and 200 GeV, respectively. The diamonds, crosses, trian-

gles, squares and circles are the experimental data of the RHIC-PHOBOS collaborations [4–6]. The solid lines are the results from Eq. (14). It can be seen from this figure that, for all four c.m.s. energies, the theoretical results are in good agreement with experimental data in the different centrality cuts at the central pseudorapidity regions. However, at large pseudorapidity regions, there exist some discrepancies between the theoretical and experimental results. These discrepancies are understandable since in our calculations we only take into account the binary nucleon-nucleon collisions. However, besides binary nucleon-nucleon collisions, the spectators and leading particles also make contributions to the final charge multiplicities, which are mainly situated at large pseudorapidity regions. Therefore, we can expect that, if the charge multiplicities from both spectators and leading particles are included, the fitting condition can be further improved.

The transverse momenta of the three major kinds of particles, namely pions, kaons and protons, have been measured in different centrality Au+Au collisions [29]. In the above calculations, the $p_{\rm T}(\boldsymbol{b})$ in Eq. (13) and Eq. (14) in each centrality cut is represented by the mean value of the transverse momenta of these three kinds of particles. The free parameter $\alpha(\boldsymbol{b})$ is fixed by fitting the experimental data. The mean numbers of effective nucleon-nucleon collisions $\bar{N}_{\rm NN}^{\rm eff}$ determined in this way are summarized in Table 2. This table shows that, in each centrality cut, $\bar{N}_{\rm NN}^{\rm eff}$ decreases with the reduction in the c.m.s energies. However, from $\sqrt{s_{\rm NN}}$=62.4 to 19.6 GeV, $\bar{N}_{\rm NN}^{\rm eff}$ seems to reach saturation. Comparing Table 2 with Table 1, one can see that the numbers of $\bar{N}_{\rm NN}^{\rm eff}$ are much smaller than those of $\bar{N}_{\rm NN}$, and with the decrease in the centrality (or impact parameter), the reduction rate of $\bar{N}_{\rm NN}^{\rm eff}$ increases. This means that a participant will lose a great part of its energy in nucleus-nucleus collisions, especially in central nucleus-nucleus collisions.

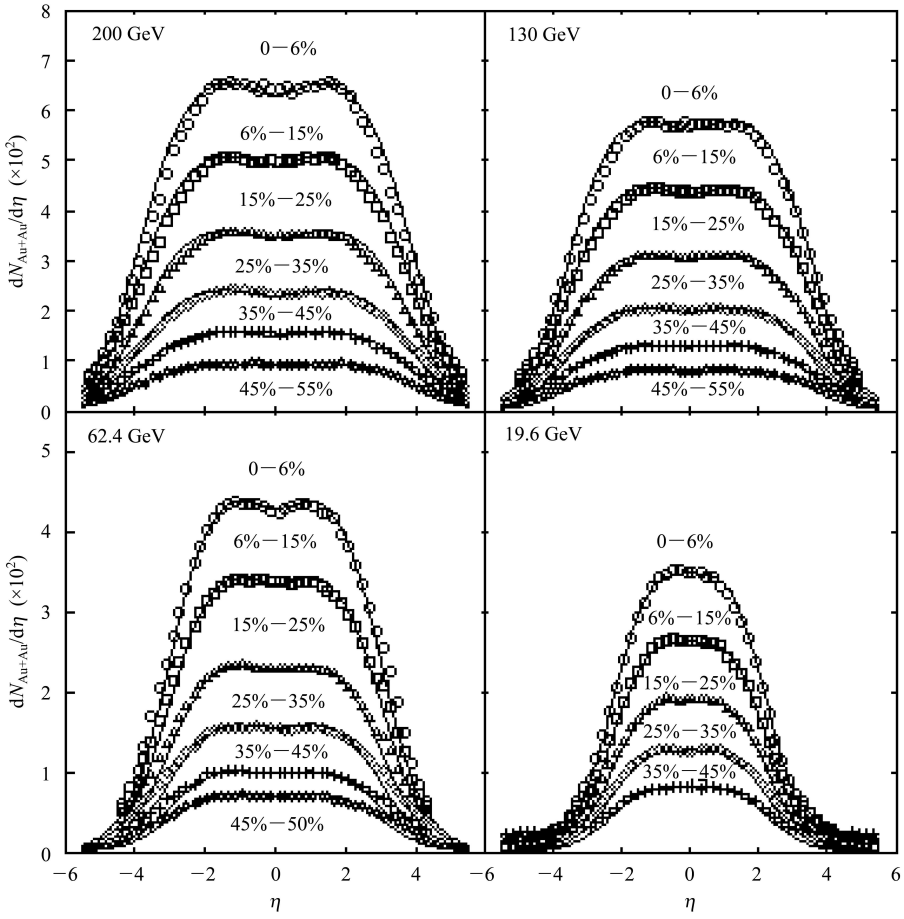

Fig. 4. Pseudorapidity distributions of charged particles for different centralities in Au+Au collisions at $\sqrt{s_{\rm NN}}$ =19.6, 62.4, 130 and 200 GeV, respectively. The diamonds, crosses, triangles, squares and circles are the experimental data of the RHIC-PHOBOS collaborations [4–6]. The solid lines are the results from Eq. (14).

Table 2. The mean numbers of effective nucleon-nucleon collisions $\bar{N}_{\rm NN}^{\rm eff}$ for five centrality cuts in Au+Au collisions at $\sqrt{s_{\rm NN}}$=19.6, 62.4, 130 and 200 GeV, respectively.

centrality cuts (%)	$\bar{N}_{\rm NN}^{\rm eff}(19.6)$	$\bar{N}_{\rm NN}^{\rm eff}(62.4)$	$\bar{N}_{\rm NN}^{\rm eff}(130)$	$\bar{N}_{\rm NN}^{\rm eff}(200)$
0–6	218	219	254	270
6–15	167	173	198	212
15–25	120	118	139	150
25–35	81	81	92	101
35–45	52	51	59	66

4 Conclusions

By using the Glauber model, we give the centrality dependences of the numbers of participants and binary nucleon-nucleon collisions in heavy-ion collisions. The calculated results are very consistent with those given by the RHIC-PHOBOS collaboration in different centrality Au+Au collisions at $\sqrt{s_{\rm NN}}$=19.6, 62.4, 130 and 200 GeV. We then present the pseudorapidity distributions of the charged particles in nucleus-nucleus collisions as a function of the beam energy and impact parameter. Owing to the energy loss of the participants in their multiple collisions, the contributions to the yield of charged particles from binary nucleon-nucleon collisions will become less and less, along with the increase in $N_{\rm NN}(\boldsymbol{b})$. To describe this fact, we introduce an attenuation factor $\beta(\boldsymbol{b})$ and use the effective number $N_{\rm NN}^{\rm eff}(\boldsymbol{b})$ to replace the real $N_{\rm NN}(\boldsymbol{b})$. As a result, the charge multiplicities in nucleus-nucleus collisions are expressed as a weighted superposition of those in effective binary nucleon-nucleon collisions. The distinguishing features of our model are a few free parameters (only $N_{\rm NN}^{\rm eff}(\boldsymbol{b})$ or $\alpha(\boldsymbol{b})$ or $\beta(\boldsymbol{b})$), straightforward from the physical picture behind and simple in its mathematical treatment. In analyzing the centrality dependence of the pseudorapidity distributions of charged particles in different centrality Au+Au collisions at $\sqrt{s_{\rm NN}}$ =19.6, 62.4, 130 and 200 GeV, we find that the theoretical model is in good agreement with the experimental observations of the RHIC-PHOBOS collaboration.

References

1 Bjorken J D. Phys. Rev. D, 1983, **27**: 140–151
2 Munzinger B P, Stachel J, Wessels J P, XU N. Phys. Lett. B, 1995, **344**: 43–48
3 Munzinger B P, Stachel J, Wessels J P, XU N. Phys. Lett. B, 1995,**365**: 1–6
4 Back B B, Baker M D, Barton D S et al (PHOBOS collaboration). Phys. Rev. Lett., 2003, **91**: 052303
5 Back B B, Baker M D, Ballintijn M et al (PHOBOS collaboration). Phys. Rev. C, 2006, **74**: 021901
6 Back B B, Baker M D, Ballintijn M et al (PHOBOS collaboration). Nucl. Phys. A, 2005, **757**: 28–101
7 Back B B, Baker M D, Ballintijn M et al (PHOBOS collaboration). Phys. Rev. Lett., 2005, **94**: 082304
8 Alver B, Back B B, Baker M D et al (PHOBOS collaboration). 2007, arXiv:0709.4008vl[nucl–ex]
9 Back B B, Baker M D, Ballintijn M et al (PHOBOS collaboration). Phys. Rev. Lett., 2004, **93**: 082301
10 Bearden I G, Beavis D, Besliu C et al (BRAHMS collaboration). Phys. Rev. Lett., 2002, **88**: 202301
11 Adams J, Aggarwal M M, Ahammed Z et al (STAR collaboration). Phys. Rev. C, 2004,**70**: 064907
12 Adare A, Afanasiev S, Aidala C et al (PHENIX collaboration). Phys. Rev. Lett., 2008, **101**: 162301
13 WONG C Y. Phys. Rev. C, 2008, **78**: 054902
14 Ryblewski R, Florkowski W. Phys. Rev. C, 2008, **77**: 064906
15 Boż ek P. Phys. Rev. C, 2008, **77**: 034911
16 LIU L S, MENG T C. Phys. Rev. D, 1983, **27**: 2640–2647
17 CHOU K C, LIU L S, MENG T C. Phys. Rev. D, 1983, **28**: 1080–1085
18 LIU F H. Phys. Rev. C, 2002, **66**: 047902
19 Hwa R C, YANG C B, Fries R J. Phys. Rev. C, 2005, **71**: 024902
20 SHAO F L, YAO T, XIE Q B. Phys. Rev. C, 2007, **75**: 034904
21 Sorge H. Phys. Rev. C, 1995, **52**: 3291–3314
22 SA B H, CAI X, SU Z D, TAI A, ZHOU D M. Phys. Rev. C, 2002, **66**: 044902
23 DONG Y F, JIANG Z J, WANG Z W. Chinese Physics C, 2008, **32**: 259–263
24 Glauber R J. In lectures in Theoretical Physics. New York, 1959, 315–322
25 WONG C Y. Introduction to High-energy Heavy-ion Collisions. Harbin: Harbin Institute of Technology Press, 2002. 222–230(in Chinese)
26 DE B, Bhattacharyya S. Phys. Rev. C, 2005, **71**: 024903
27 Werner K. Phys. Rep., 1983, **232**: 87–299
28 WONG C Y. Phys. Rev. D, 1984, **30**: 961–971
29 Adler S S, Afanasiev S, Aidala C et al (PHENIX collaboration). 2003, arXiv: 0307022vl[nucl-ex]
30 Alner G J, Ansorge R E, Å sman B et al (UA5 collaboration). Z. Phys. C, 1986, **33**: 1–6
31 ThomèW, Eggert K, Giboni K et al. Nucl. Phys. B, 1977, **129**: 365–389
32 Busza W. Acta Phys. Pol. B, 2004, **35**: 2873–2894